Numerical Analysis of the Thermodynamic Response of a Hollow Concrete Cylinder

T. T. Akano[1], H. O. Onovo[2*], O. S. Osasuyi[3], S. A. Alabi[4]

[1]Department of Mechanical Engineering, University of Botswana, Gaborone, Botswana
[2]Department of Metallurgical & Materials Engineering, University of Lagos, Lagos, Nigeria
[3]Department of Systems Engineering, University of Lagos, Lagos, Nigeria
[4]Department of Civil Engineering, University of Botswana, Gaborone, Botswana

ABSTRACT: The stability and durability of concrete materials are essential factors in the construction industry. Environmental conditions, such as temperature affect the tensile strength and durability of concrete structures. This work investigates the thermodynamic behaviour of hollow cylindrical concrete using the finite element method (FEM). By deploying ANSYS®, the element mesh was created, and the temperature distribution inside the hollow cylinder was calculated. The effect of the hollowness of the concrete on its heat absorption is determined. The findings demonstrate that the temperature profiles changed radially throughout the concrete thickness. Moreover, it was discovered that the temperature distribution was impacted by the airflow into the cylinder. The numerical experiment in this study was essential in providing a comprehensive understanding of the behaviour of the concrete, particularly when exposed to higher heating rates. This study contributes to the knowledge of the performance and stability of concrete materials. It also demonstrates that the hollowness of the concrete enhances its heat-shielding performance. Furthermore, the inflow of air into the cylinder affects the temperature distribution, with a higher influx of air resulting in lower temperatures. These findings can be utilised to develop appropriate measures to enhance the performance and durability of concrete structures.

KEYWORDS: porous materials, hollow cylinder, concrete, temperature, ANSYS®

[Received Oct. 5, 2023; Revised Nov. 2, 2023; Accepted Nov. 28, 2023] Print ISSN: 0189-9546 | Online ISSN: 2437-2110

I. INTRODUCTION

Porous media such as concrete subjected to high temperatures have been of significant consideration in the engineering profession, especially in civil engineering, for the setting up of infrastructures such as high-rise buildings, pipelines, bridges, and nuclear boats. The difference between high-performance concrete (HPC) and ordinary concrete (OC) could be ascertained in their usability. According to Witek *et al*. (2007), HPC is more durable and stronger than OC, not only because they are less permeable but also because their capillary and pore structures are relatively disjointed as a consequence of dehydration. Also, concrete's response to heat greatly matters in engineering applications (Ranc *et al*., 2001), as high-temperature range alters the porous structure of concretes (Dal Pont, Schrefler and Ehrlacher, 2005), considerably affecting its durability. Moreover, Feraille-Fresnet *et al*. (2003) stated that the microstructure and conveyance properties are modified by dehydration, producing free fluid. During this process, heat is consumed to a sizable aggregate, according to Bazant and co. (1982; 1988; 1993). Also, they stated that penetrability has an abrupt gain above 105^{o}C when drying starts. Notwithstanding, porous materials have extensive use in engineering applications such as insulation, filtration, biomedical engineering, catalysis, construction, automotive application, oil and gas sector, environmental radiation and electronics. For this reason, different experiments have been conducted to harness the full potential of such substances' characteristics. Over the decades, researchers and scientists have made considerable analyses on the optimization of porosity, surface area, and structural properties, aiming to enhance the performance and efficiency of porous materials in various applications.

The thermoelastic behaviour of functionally graded concrete rings with homogenous thermal mass and non-uniform irregular mechanical loads was studied by Rad (2015). The work presented novel findings on the thermodynamic response of an axisymmetric hollow concrete cylinder, which could be a benchmark for future researchers. Manthena *et al*. (2017) measured the thermal propagation and loadings of a cylinder with holes, as well as the quality of non-uniform elements and joule heating. This study contributes to the advancement of the role of material inhomogeneity in determining the thermal and mechanical behaviour of structures. As an extension of the work, Manthena and Kedar (2018) reviewed the results of heat separation and heat stress distribution of a reinforced composite thick circular tube with composite heat parameters, discovering that all composite attributes were a function of temperature and spatial position along the thickness of the tube, z. Using information from the heat flux within biothe cylinder, Kedar and Deshmukh (2015) exploited the reversed thermal performance problem to

*Corresponding author: honovo@unilag.edu.ng

doi: http://dx.doi.org/10.4314/njtd.v18i4.2076

concurrently predict the heat transfer displacement on the exterior curving face of a moderate cylinder with holes. According to the study, the Poisson ratio is unaffected by temperature when studying porcelain-reinforced composite materials where Alumina is used as the nickel and ceramic is used as the metal. Walde *et al*. (2012) used the integral equation technique as data analysis to obtain the temperature profile, deflection, and load functions at every location of the hollow cylinder, resulting in a way to solve the transitory thermo-elastic issue of a limited-dimension hollow cylinder. In the same way, Gahane *et al*. (2012) selected the integral transformation technique for studying the thermomechanical behaviour of a confined cylinder with holes. As a direct result of thermal and initial conditions of the emission type, the origins are considered non-spontaneous.

Under steady-state temperature gradients, a finite element study of 3D curved non-planar fractures in functionally graded materials was performed and reported by Mughaddam and Alfano in their paper (Moghaddam and Alfano, 2015). The computing method and interaction energy integral used in the research do not call for any prior understanding of the fracture front or surface curvatures. The impact of graded mechanical and thermal characteristics on stress intensity factors is investigated, demonstrating the strength of the suggested framework for examining thermal fracture in functionally graded materials (FGMs). In his research, Zhang (2018) proposed a stress and displacement solution method for analysing cylindrical structures with varying material properties under non-uniform pressures. The method is based on elastic mechanics and can be applied to different contact conditions. The proposed solution is validated through numerical simulations, laying a theoretical foundation for stress analysis and structural design in practical engineering.

In order to increase the U-value without modifying the compressive strength, size, or manufacturing procedure, Caruana *et al*. (2017) examined the thermal characteristics of a novel hollow-core concrete construction block. The study illustrates the validity of in-situ testing procedures for assessing the thermal characteristics of building components without needing a hot box setup in a laboratory. Using theoretical and numerical methods, Bi-chao and Hao (2019) analysed the thermal characteristics of tiny hollow concrete blocks with various hole size types. The optimal block structure for thermal insulation and heat-shielding performance is determined, and the relationship between block structure parameters and thermal properties was examined. To determine which was stronger, Hasan *et al*. (2021) evaluated brick masonry walls, standard reinforced concrete beams, and columns against hollow concrete block masonry walls, beams, and columns. The results showed that reinforced hollow concrete block masonry walls are stronger than brick-built ones and that reinforced hollow concrete block reinforced beams have greater flexural and shear capacity and flexural ductility than conventional reinforced concrete beams.

The criteria for assessing the mechanical characteristics of concrete blocks under high temperatures was examined by Medeiros *et al*. (2022). The study recommended the variables needed for a laboratory assessment of residual mechanical strength at high temperatures. It also recommends assessing the residual mechanical strength of hollow concrete blocks, including the quantity of specimens, the age of the test subjects, the storage conditions, and the rate at which the temperature rises during heating. Debska *et al*. (2022) examined how pre-stressed nickel-titanium (Ni-Ti)-shape memory alloy (SMA) wires wrapped around concrete cylinders with holes responded to stresses. Two models were used to determine the thermal stresses in the concrete and the loads caused by the wrapped wire. Longitudinal compression tests were carried out one year after pre-stressing, and the results showed that the technique was effective.

Using the finite-difference approach, Miroshnichenko *et al*. (2022) provided a computational solution for resolving the issue of heat transmission in hollow blocks. Also presented is the process for thickening the computing grid. According to the study, hollow bricks have a turbulent flow regime, and the inner surfaces' emissivity significantly influences how much heat is transmitted through them. Jamal *et al.* (2021) numerically analysed the three categories of hollow bricks' thermal behaviour commonly utilised in Moroccan building walls. The effects of thermal excitation, emissivity, and period on heat transfer through the structures are studied. The outcomes show that type 3 hollow bricks provide good insulation and materials with a low emissivity for interior surfaces can improve energy consumption in buildings.

Researchers have adopted numerical and hybrid approaches to analyse composite and concrete cylinders. Dehghan *et al.* (2022) proposed a new mixed method combining the Fast Fourier Transform (FFT) and FEM to study the thermo-mechanical performance of functionally graded cylinders under asymmetric loading. The technique shows super algebraic convergence in the circumferential direction and benefits from fast convergence and low computational cost compared to the FEM solution. Considering radiation effects, Kogawa *et al*. (2017) examined turbulent natural convection in a cubic hollow space. The research used large eddy simulation and a coupled calculation method to efficiently calculate thermal radiation flux. The impact of surface radiation was found to be more dominant than the gas radiation effect in flow instability and shear stress generation.

The influences of radiation and convection on the thermal surroundings in an industrialised facility were studied by Wang *et al.* (2014). The study focuses on control parameters, including Grashof numbers and surface emissivity values. Results for ventilation rate, flow distributions, heat transfer and temperature are provided. The Grashof number negatively correlates with the radiation-to-convection ratio, while the surface emissivity has a positive correlation. On the other hand, the ventilation rate and Nusselt number are both rising functions of these variables. The combined impact of CO_2 production mixed turbulent convection with thermal radiation, and human heat creation on interior comfort and energy utilisation in buildings was examined by Rodriguez *et al.* (2013). The findings indicate that thermal radiation raises average temperatures by 0.2–0.4°C, whereas natural ventilation lowers them by 4.0–5.5°C. Rahimi and Sabernaeemi (2010, 2011) looked at how radiation and convection affected the transport of heat from a heated ceiling surface to interior surfaces in a space. Results show that over

90% of heat transfer occurs through radiation, and this contribution increases slightly as the ceiling temperature rises. In a large-scale chamber containing a thermally-generating device, Miroshnichenko *et al.* (2021) computationally modelled turbulent thermogravitational convection and thermal radiation.

Pertaining to heat transfer and fluid motion, the effect of the hot source's height and wall emissivity is investigated. The findings indicate that an increase in heater height can raise the average total Nusselt number by up to two times and that the surface emissivity of the heat source greatly influences the total thermal transfer coefficient.

Based on the literature survey, it is vital to do numerical research on the heat transmission mechanisms in hollow concrete materials. Therefore, the present work focuses on the thermodynamic response of a hollow concrete cylinder. The mathematical model for the analytical procedure, numerical experiment, results, discussion of results, validation, and conclusion are presented in the subsequent sessions.

II. MATERIALS AND METHODOLOGY

A. Model Assumptions

The assumptions utilised are those specified in Dal *et al.* (2005). The medium is evaluated from a large standpoint, allowing the continua theory of a substance to be accepted, which is a common strategy in thermodynamics. It is considered that a massive volume of components is distinguishable as quantifiable metrics of atomic proportions at larger sizes. Additionally, thermodynamic equilibrium is maintained. It is also essential to know that the duration of the entire state's fluctuations is longer than required to achieve microbalance. Thus, averaged molecular attributes become crucial because the number of molecules is so large.

Due to the acceptance of local thermodynamic assumptions, a slow process was considered. To consider the porous material's characteristics as a continuous function of the spatial coordinates, a few more types of big-sized volume approximation are applied. Furthermore, the equilibrium equations express the agreement and/or variations of the isothermal dimensions at optimum, minimising the number of free variables required to explain the structure of the model.

B. Physics Concept of the Problem

Equilibrium equations, including conservation laws, straight and rotary momentum equilibrium laws, and thermodynamic formulae, are fundamental for describing the behaviour of a system in a state of equilibrium. These equations are supported by state equations and compositional connections that represent the unique behaviour of the considered medium. The entropy inequality must be used to provide a consistent thermodynamic description of the substance's reaction that does not deviate from the law of thermodynamics.

The averaging concept and the theory of partly saturated permeable materials are presented in detail in the work of Hassanizadeh and Gray (1979a, 1979b, 1980, 1989). The intrinsic permeability of concrete, which describes the intrusion of fluids through a permeable medium due to the flow energy of a fluid column, is a vital characteristic of the material and is established through laboratory investigation, according to Dal *et al.* (2005).

When concrete is heated, it undergoes complex reversible and irreversible reactions that result in interior transformation, increased penetrability, and increased inherent absorption. Schneider and Herbst (1989) have provided various effects on the variations in the permeability and inner structure of four distinct types of concrete mixes under intense temperatures. A substantial type of model was used to approximate the results obtained giving the intrinsic permeability, K as,

$$K = K_0 \cdot 10^{A_T^2 (T-T_0)^2 + A_{T(T-T_0)}^1} \left(\frac{p_g}{p_0}\right)^{A_p} 10^{A_U U} \quad (1)$$

Where A_T^1, A_T^2, A_p and A_U are parameters whose values cannot be easily observed, K_0 is the inherent susceptibility at zero states. T, p_0, p_g and U are the temperature, gas pressure and cumulative loss respectively. T_0 and p_0, are the ambient temperature and pressure. Eqn. (1) considers all the main phenomena causing the unfolding of intrinsic permeability, except local macrocracks. These parameters cannot be directly obtained; hence, they are set to provide a satisfactory approximate solution to the practical gas pressures.

C. Analytical Formulation

Concrete undergoes various transformations in its formation, which lead to extreme changes in its material properties when exposed to heating with a scalar isotropic pattern (Mazars, 1986). The thermo-chemical degradation parameter, Q, is a measurement of the development of Young's modulus of the mechanically intact material E_0, and it is provided as follows:

$$Q = 1 - \frac{E_0(T)}{E_0(T_a)} \quad (2)$$

where T_a is the ambient temperature and $E_0(T)$ is the impulsive undamaged material at the same temperature. The spontaneous damage parameter u can be used to calculate Young's modulus $E(T)$ at temperature, T given in Eqn. (3).

$$E(T) = (1-u)E_0(T) \quad (3)$$

The total damage parameter D has the expression,

$$D = 1 - \frac{E(T)}{E_0(T_a)} = 1 - \frac{E(T)}{E_0(T)}\frac{E_0(T)}{E_0(T_a)} = 1 - (1-u)(1-Q) \quad (4)$$

The classified adequate load conceptualisation is also altered to account for overall damage; as a result, an additional loss in the resilient region is included as a result of damage, as expressed in Eqn. (5).

$$\tilde{\sigma} = \sigma \frac{X}{\tilde{X}} = \frac{\sigma}{(1-u)(1-Q)} \quad (5)$$

The expression for the non-local damage parameter involves several key terms. The overall area of the damaged material is denoted by X, while the impenetrable area is denoted by $\tilde{X}$. The theoretical stress tensor is represented by σ, while the altered efficient stress tensor is denoted by $\tilde{\sigma}$. The overall area of the damaged material, X, is the total area of the material that has undergone damage, while the impenetrable area, $\tilde{X}$, represents the area of the material that is still intact and has not undergone any damage. The theoretical stress tensor, σ, represents the stress within the material under ideal conditions, while the altered efficient stress tensor, $\tilde{\sigma}$, considers the influence of damage on the material's stress state. The non-local damage parameter measures the extent of

damage in the material and is essential in predicting the material's failure under different loading conditions. The relevant form of elastic energy is derived from the definition of the changed effective stress, thus;

$$\rho\psi_e = \frac{1}{2}(1-u)(1-Q)\Lambda_0 : \varepsilon^e : \varepsilon^e \quad (6)$$

Here, the rigidity tensor of the intact material is Λ_0. The fatigue relationship is written as:

$$\sigma = (1-u)(1-Q)\Lambda_0 : \varepsilon^e = (1-\mathrm{U})\Lambda_0 : \varepsilon^e \quad (7)$$

while the discharged energy rate W is given as:

$$W = -\frac{\partial(\rho\psi_e)}{\partial \mathrm{U}} : \varepsilon^e : \varepsilon^e = \frac{1}{2}\Lambda_0 : \varepsilon^e : \varepsilon^e \quad (8)$$

The damage index can be split into two portions based on the different performances of concrete in compression and tension, viz u_c and u_t respectively. They are both functions of the average equivalent strain that is determined from Eqn. (9) as follows:

$$\sigma_i = \left\{\frac{\kappa_0(1-A_i)}{\bar{\varepsilon}} + \frac{A_i}{exp[B_i(\bar{\varepsilon}-\kappa_0)\, g(\varepsilon_i)]}\right\} E\varepsilon_i \quad (9)$$

Here, the function $g(\varepsilon_i)$ is a rectification feature that considers the effect of previous loading history on material behaviour, and κ_0 is the original value of the hardening/softening parameter. The expression for the maximum tensile stress, $f_t(T)$, is given as;

$$f_t(T) = g(\varepsilon_i)\,.\kappa_0 \quad (10)$$

The value of κ_0 is chosen such that it satisfies the De Saint-Venant's principal strain requirement, as stated in Eqn. (11).

$$f(\kappa_0, \varepsilon, \Lambda) = \bar{\varepsilon} - \kappa(\mathrm{D}) \quad (11)$$

In the non-local approach to damage theory, the comparable strain over a hypothetical volume is defined as the average strain. This hypothetical volume is often referred to as the "metaphorical volume". The comparable strain is determined by considering the effect of surrounding material points on the deformation at a given point. This approach takes into consideration the non-local behaviour of the material, which occurs when the behaviour of the material at one location is impacted by the behaviour of material points nearby. Therefore, the comparable strain is not limited to the deformation at a single point but considers the deformation of the material in the surrounding vicinity. The average comparable strain over the metaphorical volume is defined as:

$$\bar{\varepsilon} = \frac{1}{V_r(x)}\int_v \zeta(x-s)\ \tilde{\varepsilon}(s)dv \quad (12)$$

where ζ is a sampling distribution and $\propto_t$ is a time interval. $\tilde{\varepsilon}$ is the damage progress determined by the comparable positive strain given in Eqn. (13).

$$\tilde{\varepsilon} = \sqrt{\sum(<\varepsilon_i>_+)^2}\left(<\varepsilon_i>_+ = \frac{|x|+x}{2}\right) \quad (13)$$

Finally, the structural damage is calculated using the aggregate:

$$u = \propto_t u_t + \propto_c u_c \quad (14)$$

where $\propto_t$ and $\propto_c$ are defined in Eqn. (15) thus,

$$\propto_t = \sum_{i=1}^{3}\left(\frac{\varepsilon_{ti}<\varepsilon_i>_+}{\tilde{\varepsilon}^2}\right)^{\beta} \ ; \ \propto_c = \sum_{i=1}^{3}\left(\frac{\varepsilon_{ci}<\varepsilon_i>_+}{\tilde{\varepsilon}^2}\right)^{\beta} \quad (15)$$

Heat parameters, or material properties, are A_t, A_c, B_t, B_c. The index β compensates for the influence of damage on the material's shear behaviour. The function $g(\varepsilon)$ takes the form:

$$g(\varepsilon_c) = \left(\frac{\kappa_0 - \varepsilon_c}{\kappa_0 - \varepsilon_{c\,max}}\right)^{\gamma} \quad (16)$$

In this study, the maximum allowable strain, denoted by $\varepsilon_{c\,max}$ was determined to be the distortion that corresponds to a load equal to the compressive strength test. To quantify the maximum allowable strain, a variable γ was introduced, which is a product of B_c and $\varepsilon_{c\,max}$. Additionally, the tensile strain at which damage occurs at a specific temperature denoted as $\kappa_0(T)$, was investigated. This phenomenon was analysed using Mazars' model (Mazars, 1986), which postulates that damage occurs when the maximum tensile stress, $f_t(T)$, is reached under uniaxial stress conditions. The expression for $f_t(T)$ is given by;

$$\kappa_0(T) = \frac{f_t(\mathrm{T})}{E_0(T)} \quad (17)$$

III. NUMERICAL EXPERIMENT

In this study, the FEM was utilised to discretise a hollow cylinder, enabling a high degree of flexibility in defining the mesh. Specifically, a hollow cylinder was considered, with internal and external radii of $R_1 = 0.25m$ and $R_2 = 0.55m$, respectively. The temperature boundary condition was set to $T_a = 293.15K$ ambient temperature. The dimensioned hollow with the boundary condition is shown in Figure 1.

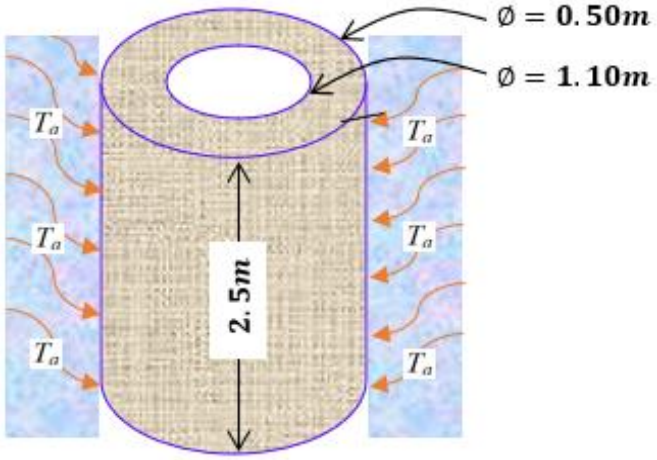

Figure 1: Hollow Cylindrical Concrete

To precondition the analysis, we specified an internal surface air velocity of $v_{in} = 1.39m/s$ and assumed atmospheric pressure at the outer surface. Furthermore, the inner part of the pipe was assumed to be subjected to laminar flow, while the external part was treated as time-dependent. This approach allowed for the investigation of the dynamic behaviour of the system under thermal loading. The thermal rate of loading was applied 70 $hours$, starting from an initial temperature of $293.15K$, which is the room temperature. During this period, the outer layer of the cylinder was allowed to freely exchange heat with the surrounding environment.

For a proper analysis of the problem, it is essential to have a properly defined geometric model of the hollow cylindrical concrete structure. This was achieved by creating the geometry directly in ANSYS using its modelling capabilities. The model accurately represents the dimensions and features of the structure, including the inner and outer diameters and wall thickness. To generate the finite element mesh ANSYS is deployed. ANSYS offers various meshing techniques,

including automatic and manual methods. A shell element is used to model the walls for the hollow cylindrical concrete structure. The mesh model, as generated by ANSYS, is shown in Figure 2. The cylinder is discretised into 1008 prismatic meshes. This technique makes it possible to investigate the thermal behaviour and stress distribution in a hollow cylinder under diverse circumstances, which has real-world engineering implications.

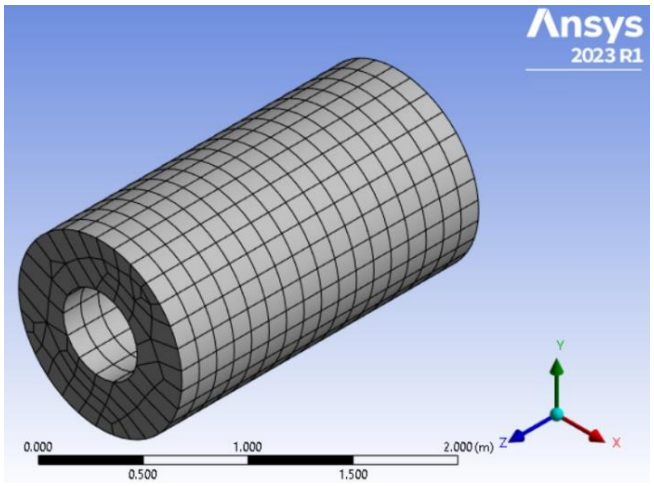

Figure 2: Meshed Hollow Cylindrical Concrete

In the current work, concrete's material characteristics at room temperature are analysed, emphasising the temperature profile of hollow concrete. The experimental results shown in Table 1 depict that the hollow concrete has considerably high average compressive and tensile strengths, which denotes a high resilience. This finding is in line with earlier studies in the area.

Table 1: Material properties of the concrete

Parameter	Symbol	Value	Unit
Poisson ratio	ν	0.18	
Heat capacity	C_p	855	$J/kg.K$
Coefficient of thermal expansion	$\propto$	10 x10^{-6}	$1/K$
Intrinsic permeability	K	2 x10^{-17}	m^2
Thermal conductivity	C	1.52	$W/m^2\,K$
Young's modulus	E	36.70	GPa
Porosity	n	0.051	
Tensile strength	f_t	6.0	MPa
Apparent Density	ρ	2620	kg/m^3
Compressive strength	f_c	109	MPa

IV. RESULTS AND DISCUSSION

An FEA was carried out to get the temperature field to further examine the behaviour of the concrete portion under consideration. To replicate the section's thermal behaviour for this investigation, finite element meshes were used. After that, the study's findings were used to learn more about the concrete structure's thermomechanical behaviour at temperatures other than the ambient one. Researching the material characteristics of concrete and the thermal behaviour of concrete buildings is a demanding and scientific procedure. Figure 3 depicts the temperature distribution along hollow cylindrical concrete.

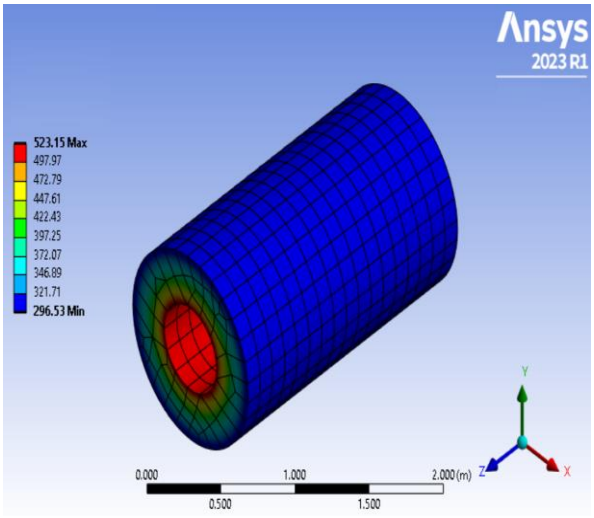

Figure 3: Temperature Distribution along Hollow Cylindrical Concrete

Figure 4(a) depicts the temperature field in a hollow concrete after 70 hours, which is a 2-dimensional contour. The resulted from a study utilising finite elements of the temperature distribution over the concrete thickness. The mean temperature was discovered to be higher in the void closest to the wall than in the void further away, proving that the dispersion of temperature changed radially across the thickness of the concrete.

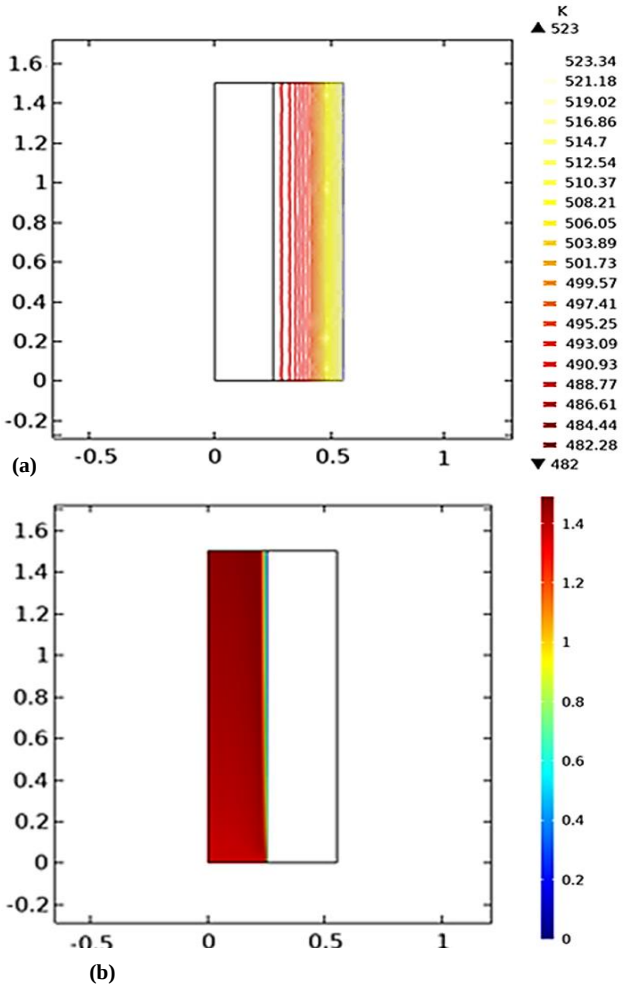

Figure 4: 2D contour view of the (a) temperature profile (b) velocity profile in the hollow cylinder after 70 hours

The observed temperature variation is mainly ascribed to fluid flow and heat transfer processes resulting from the transfer of energy from the lower to the upper vacuum, aligning with the findings of Ibrahim *et al*. (2023). In addition to temperature distribution, the radial velocity and pressure variations across the hollow cylinder were also analysed. Figure 4 (b) illustrates that the velocity decreases radially while the pressure is higher at the hole inlet and decreases along the length of the hollow cylinder. These observations provide valuable insights into the heat transfer and fluid flow processes occurring in the concrete sample. They can aid in developing effective heating and cooling strategies for concrete structures.

The mass flow of air in a void sample was found to follow the same pattern at each location due to the geometry resolution, besides the right and left side's outside walls being heated and cooled. The analysis leads to the conclusion that increasing the thickness of the concrete is imperative to attain a heat resistance level consistent with the findings of Balaji *et al*. (2016).

To ensure that all the concrete surfaces were heated uniformly during the validation process, two points at the top and bottom of the cylinder were considered. The temperature measurements obtained from two distinct locations on the heating sample are graphed in Figure 5. The graph depicted a consistent rate of temperature increase over time, with the top of the cylinder exhibiting an approximate increase of 3.3 K/hr and the bottom showing a rate of approximately 2.7 K/hr. These observations were made after subjecting the sample to 70 hours of thermal exposure. Additionally, the temperature values acquired at each of the two readings with the heated sample highlight the observed temperature variations.

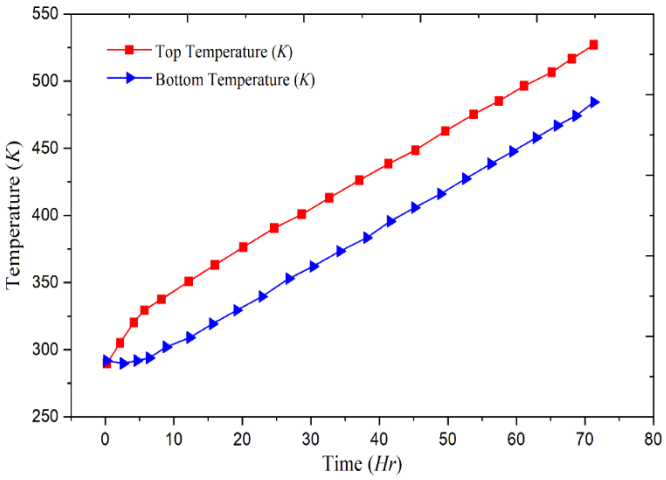

Figure 5: Time history of temperature

Based on the results presented in Figure 5, it can be inferred that the sample was heated evenly, indicating the effectiveness of the heating method adopted. The sample heating process must sustain precise temperature control throughout the exposed surface of the concrete to ensure accurate and reliable results. Figure 5 displays the temperature readings acquired at the two measurement points after heating the sample. The readings at the two points show a distinct difference, almost forming a parallel increment after the initial parabolic departure. This temperature distribution pattern suggests that heat transfer occurred uniformly across the surface of the concrete sample, indicating a homogeneous temperature distribution.

The modelling of internal voids is important during the temperature evolution in structural elements. In addition, the insulation index is one function that describes the material's thermal efficiency. Because the thermal conductivity of air is lower than that of the other components that make up the material structure, the air layer helps to prevent heat transfer within a particular layer. When the airflow covering reaches a particular thickness, the thermal insulation coefficient of the air layer does not significantly increase due to the increasing thermal transfer gap. Therefore, the hollowness of the concrete gives the best heat-shielding performance, as can be seen from the temperature response in Figure 5. Where there is a high inflow of air, the temperature is low. Hence, enhancing thermal insulation performance is achievable by reducing the void ratio, as this action results in increased air pressure due to the inverse relationship between volume and pressure.

The modelling of internal voids is important during the temperature evolution in structural elements. In addition, the insulation index is one of the functions that describe the material's thermal efficiency. Given that air has a lower thermal conductivity compared to the other constituent materials in the structure, an air layer can serve as a barrier to prevent heat transfer across a given layer. As the thickness of the air layer increases, the thermal insulation coefficient of the layer does not significantly improve due to the increased thermal transfer gap. Based on the velocity profile illustrated in Figure 4(a), it can be inferred that the hollowness of the concrete provides the best heat-shielding performance. It is observed that a higher airflow rate leads to a lower temperature, which highlights the importance of reducing the hollow ratio. Decreasing the hollow ratio of the concrete increases the pressure of the air, which subsequently enhances the thermal insulation performance. This is attributed to the fact that a decreased volume leads to an increased pressure of the air, which effectively reduces the thermal conductivity and thus improves the overall thermal insulation performance of the material (Yarbrough, 2012; Wakisaka *et al.*, 2016; Christiansen *et al.*, 2022).

The current study builds on the previous work conducted by other researchers (Li, Zhou and Duszczyk, 2004; Liu, Zhou and Duszczyk, 2007) to explore the correlation between top temperature and air velocity for concrete materials. The variation of temperature along the concrete thickness is shown in Figures 6 and 7 with $t = 20h$ and $t = 40h$, respectively. The experimental result validates the present study R^2 values of 0.9786 when $t = 20h$ and 0.9735 and $t = 40h$. A nonlinear decrease in temperature is observed along the radius profile of the cylinder. The impact of airspeed on the top temperature of the hollow concrete cylinder during the thermodynamic process is illustrated in Figure 8. The mathematical model developed by this work predicts the correlation between top temperature and air velocity as $T(K) = 728.4(K) - 60.25 \times v(m/s)$. The result demonstrates a decrease in top temperature with an increase in air velocity, which is consistent with the findings of Acharya and Dash (2017).

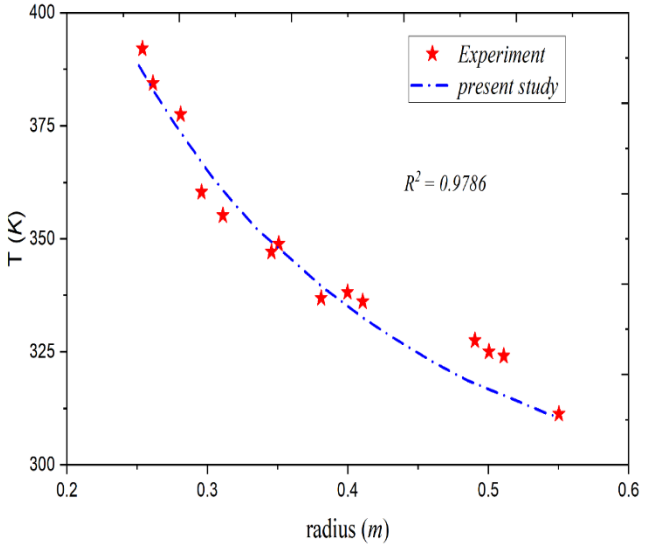

Figure 6: Temperature profile along the concrete radius when time, $t = 20h$

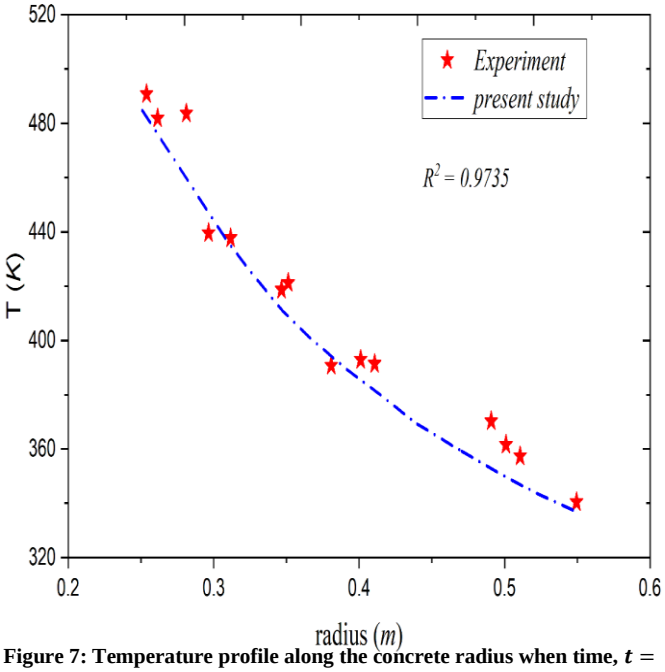

Figure 7: Temperature profile along the concrete radius when time, $t = 40h$

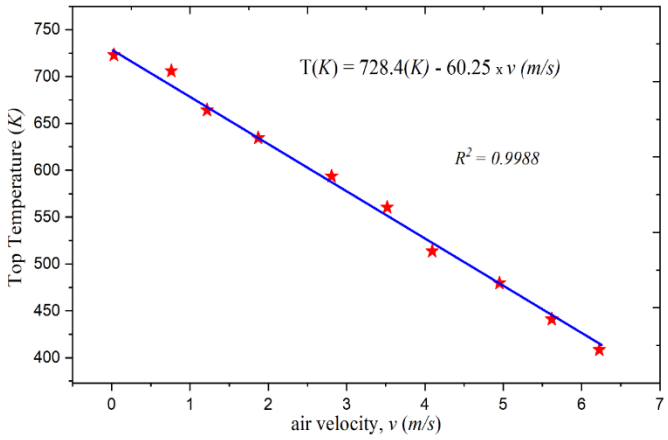

Figure 8: Effect of airflow on the top temperature

Investigating the temperature profiles of a hollow concrete cylinder was the goal of the current analysis during the thermodynamic process and compare the outcomes with experimental results. The obtained temperature profiles were found to align well with experimental outcomes, as illustrated in Figure 9. A front of desaturation and molecular migration to the colder zones were the defining features of the physical events operating inside the cylinder. It was observed that the numerical temperature distribution solution should not materially differ from the analytical result proposed by Liu *et al*. (2007), given the low water content of the concrete. The result obtained through numerical simulations, as presented in Figure 9, corroborated the analytical approach. Moreover, the temperature profile exhibited a satisfactory agreement with the experimental result obtained by Dal *et al*. (2005).

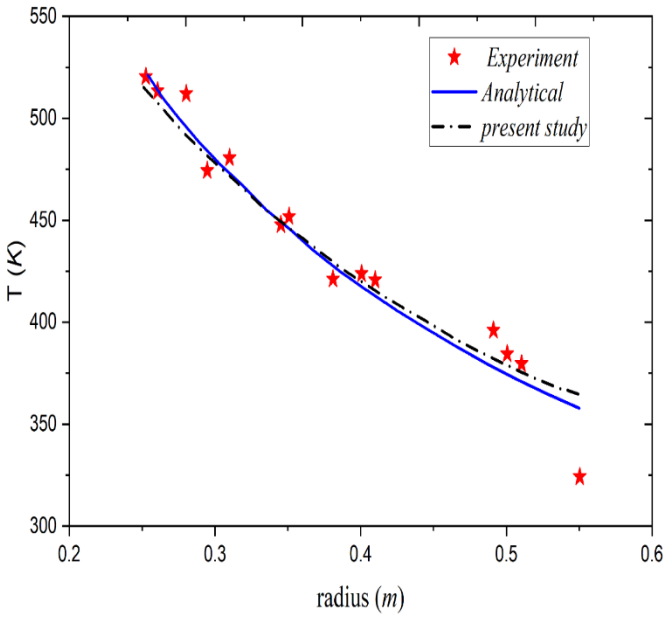

Figure 9: Temperature profile with the analytical solution along the concrete radius

However, it should be noted that the intricacy of this analysis is acceptable when higher heating rates of about 7.8 K/hr are considered. In such cases, the numerical experiment becomes essential to adequately describe the behaviour and performance of the concrete. Therefore, this research's findings are of particular significance when examining the thermal behaviour of structural elements under varying temperature conditions.

Error analysis of both the analysis and present study with the experimental result is shown in Figure 10. The absolute errors between the experiment and analytical values range from 0.44618% and 4.72233%. In comparison, the absolute errors between the experiment and the numerical values range from 0.52907% and 4.04238%. The measured values from the experiment result generally conform with both the expected values obtained from the analytical model and the numerical method. The relative errors for both the analytical and numerical methods vary with different radius values.

These values, in some cases, are similar, indicating that both approaches provide a comparable level of accuracy. Minor errors are observed for the radius measurements (e.g.,

0.3449, 0.40992), indicating a closer agreement between the experiment and theoretical values.

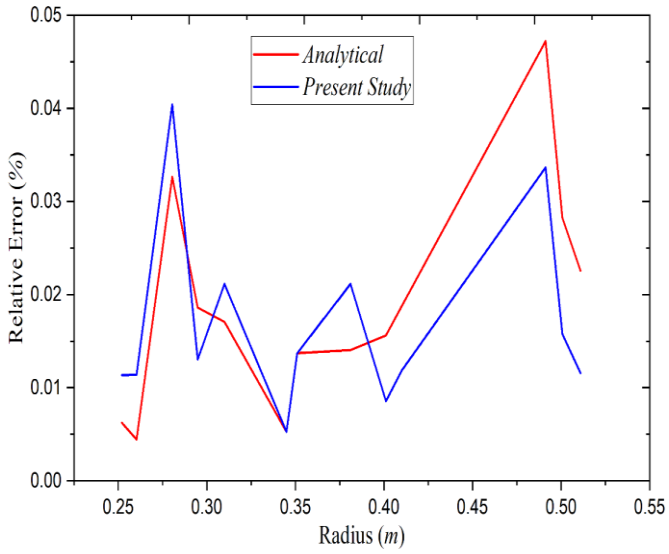

Figure 10: Error analysis of both the analysis and present study with the experimental result

V. CONCLUSION

This study investigated the thermal behaviour of hollow cylinders through finite element analysis (FEA) using the ANSYS® Multiphysics. The results obtained were validated using analytical and experimental procedures, indicating good agreement between the temperature distributions. Specifically, the temperature dissipation increased with time but decreased radially. Experimental investigations effectively produce satisfactory results when conducted under normal temperature conditions. However, numerical investigations can be more cost-effective and less risky when dealing with elevated temperatures. Therefore, this research holds significant potential benefits for the moulding and casting industries, particularly in the context of the extrusion process.

The implications of the findings of this research are significant for the design and construction of concrete structures, particularly in terms of improving their resilience and durability. In addition, the relationship between mechanical properties and changes in temperature provides important insights into the stability and performance of the material. The work also shows how numerical simulation may be used to describe the thermal behaviour of permeable bodies.

In its whole, the work advances the understanding of the thermal behaviour of hollow cylinders. The knowledge gathered from this study may also guide future investigations and useful applications in materials science and engineering.

AUTHOR CONTRIBUTIONS

T. T. Akano: Conceptualization, Methodology, Software, Validation, Writing – original draft, Writing – review & editing. **H. O. Onovo**: Supervision, Writing – original draft, Writing – review & editing. **O. S. Osasuyi**: Writing – original draft, Writing – review & editing. **S. A. Alabi**: Writing – review & editing.

REFERENCES

Acharya, S. and Dash, S.K. (2017). Natural convection heat transfer from a short or long, solid or hollow horizontal cylinder suspended in air or placed on the ground. *Journal of Heat Transfer*, 139(7), 072501.

Balaji, A.; P., Nagarajan and T.M.M., Pillai (2016). Predicting the response of reinforced concrete slab exposed to fire and validation with IS456 (2000) and Eurocode 2 (2004) provisions. *Alexandria Engineering Journal*, 55(3), 2699–2707.

Bazant, Z.P. and Carol, I. (1993). Creep and shrinkage of concrete. *E & FN Spon*, 805-829.

Bazant, Z.P. and L'Hermite, R. (1988). Mathematical modeling of creep and shrinkage of concrete. J. Wiley & Sons, New York, NY, USA.

Bazant, Z.P. and Wittmann, F.H. (1982). Creep and shrinkage in concrete structures. J. Wiley & Sons, New York, 129–161.

Bi-chao, Y.E. and Zhou, H. (2019). Thermal Performance Analysis of Concrete Small Hollow Block. In *IOP Conference Series: Materials Science and Engineering*. IOP Publishing, 012-041.

Caruana, C.; C., Yousif; P. Bacher; S. Buhagiar and C. Grima (2017). Determination of thermal characteristics of standard and improved hollow concrete blocks using different measurement techniques. *Journal of Building Engineering*, 13, 336–346.

Christiansen, L.; Y. I. Antonov; R. L. Jensen; E. Arthur; L. W. de Jonge; P. Møldrup; H. Johra and P. Fojan (2022). Heat and air transport in differently compacted fibre materials. *Journal of Industrial Textiles*, 51(8), 1250–1263.

Dal Pont, S.; B. A. Schrefler and A. Ehrlacher (2005). Experimental and finite element analysis of a hollow cylinder submitted to high temperatures. *Materials and Structures*, 38, 681–690.

Dębska, A.; P. Gwoździewicz; A. Seruga; X. Balandraud and J. F. Destrebecq (2022). The Longitudinal Compression Capacity of Hollow Concrete Cylinders Prestressed by Means of an SMA Wire. *Materials*, 15(3), 826.

Dehghan, M; A. Moosaie; M. Zamani Nejad (2022). An Approximate Thermo-Mechanical Solution of a Functionally Graded Cylinder Using Hybrid Integral Transform and Finite Element Method. *Journal of Solid Mechanics*, 14(1), 17–36.

Feraille-Fresnet, A.; P. Tamagny; A. Ehrlacher and J. Sercombe (2003). Thermo-hydro-chemical modelling of a porous medium submitted to high temperature: an application to an axisymmetrical structure. *Mathematical and Computer Modelling*, 37(5–6), 641–650.

Gahane, T.T.; V. Varghese and N. W. Khobragade (2012). Transient Thermoelastic Problem of a cylinder with heat sources. *Int. J Latest Trend Math*, 2(1), 25–36.

Gray, W.G. and Hassanizadeh, S.M. (1989). Averaging theorems and averaged equations for transport of interface properties in multiphase systems. *International Journal of Multiphase Flow*, 15(1), 81–95.

Hasan, M.; T. Saidi; D. Sarana (2021). The strength of hollow concrete block walls, reinforced hollow concrete block

beams, and columns. *Journal of King Saud University-Engineering Sciences*, 34(8), 523-535.

Hassanizadeh, M. and Gray, W.G. (1979a). General conservation equations for multi-phase systems: 1. Averaging procedure. *Advances in Water Resources*, 2, 131–144.

Hassanizadeh, M. and Gray, W.G. (1979b). General conservation equations for multi-phase systems: 2. Mass, momenta, energy, and entropy equations. *Advances in Water Resources*, 2, 191–203.

Hassanizadeh, M. and Gray, W.G. (1980). General conservation equations for multi-phase systems: 3. Constitutive theory for porous media flow. *Advances in Water Resources*, 3(1), 25–40.

Ibrahim, S.; D. N. K; Marwat and N. Ullah (2023). Flow and heat transfer in a meandering channel. *Frontiers in Materials*, 10, 01-12.

Jamal, B.; M. Boukendil; L. El Moutaouakil; A. Abdelbaki Z. and Zrikem (2021). Thermal analysis of hollow clay bricks submitted to a sinusoidal heating. *Materials Today: Proceedings*, 45, 7399–7403.

Kedar, G. D. and Deshmukh, K.C. (2015). Inverse Heat Conduction Problem in a Semi-infinite Hollow Cylinder and its Thermal Deflection by Quasi-static Approach. *International Journal of Applied Mathematics and Computation*, 6(2), 15–21.

Kogawa, T.; J. Okajima; A. Sakurai; A. Komiya S. and Maruyama (2017). Influence of radiation effect on turbulent natural convection in cubic cavity at normal temperature atmospheric gas. *International Journal of Heat and Mass Transfer*, 104, 456–466.

Li, L.; J. Zhou; J. Duszczyk (2004). Prediction of temperature evolution during the extrusion of 7075 aluminium alloy at various ram speeds by means of 3D FEM simulation. *Journal of Materials Processing Technology*, 145(3), 360–370.

Liu, G.; J. Zhou; J. Duszczyk (2007). Prediction and verification of temperature evolution as a function of ram speed during the extrusion of AZ31 alloy into a rectangular section. *Journal of Materials Processing Technology*, 186(1–3), 191–199.

Manthena, V.R and Kedar, G.D. (2018). Transient thermal stress analysis of a functionally graded thick hollow cylinder with temperature-dependent material properties. *Journal of Thermal Stresses*, 41(5), 568–582.

Manthena, V.R.; N. K. Lamba and G. D. Kedar (2017). Thermoelastic analysis of a nonhomogeneous hollow cylinder with internal heat generation. *Applications and Applied Mathematics: An International Journal (AAM)*, 12(2), 946 -967.

Mazars, J. (1986). A description of micro-and macroscale damage of concrete structures. *Engineering Fracture Mechanics*, 25(5–6), 729–737.

Medeiros, W.A.; G. A. Parsekian and A. L. Moreno Jr (2022). Test methodology for determining the mechanical properties of concrete blocks at high temperatures. *Materials and Structures*, 55(2), 1-14.

Miroshnichenko, I. V.; N. S. Gibanov and M. A. Sheremet (2022). Numerical Analysis of Heat Transfer through Hollow Brick Using Finite-Difference Method. *Axioms*, 11(2), 37.

Miroshnichenko, I. V; A. A. Toilibayev and M. A. Sheremet (2021). Simulation of thermal radiation and turbulent free convection in an enclosure with a glass wall and a local heater. *Fluids*, 6(2), 91.

Moghaddam, A. S. and Alfano, M. (2015). Determination of stress intensity factors of 3D curved non-planar cracks in FGMs subjected to thermal loading. *Engineering Fracture Mechanics*, 146, 172–184.

Rad, A.B. (2015). Thermo-elastic analysis of functionally graded circular plates resting on a gradient hybrid foundation. *Applied Mathematics and Computation*, 256, 276–298.

Rahimi, M. and Sabernaeemi, A. (2010). Experimental study of radiation and free convection in an enclosure with a radiant ceiling heating system. *Energy and Buildings*, 42(11), 2077–2082.

Rahimi, M. and Sabernaeemi, A. (2011). Experimental study of radiation and free convection in an enclosure with an under-floor heating system. *Energy Conversion and Management*, 52(7), 2752–2757.

Ranc, G.; J. Sercombe; S. Rodrigues and C. Gatabin (2001). Structural and local behaviour of reinforced high-strength mock-up subjected to high temperatures. In *Conf. Int. FRAMCOS*, 28.

Rodriguez Muñoz, N.A.; Z. C. Briceño Ahumada; J. F Hinojosa Palafox (2013). Numerical study of heat transfer by convection and thermal radiation in a ventilated room with human heat generation and CO_2 production. *Latin American Applied Research*, 43(4), 353–361.

Schneider, U.and Herbst, H. (1989). Permeability and porosity of concrete at high temperature. *Deutscher Ausschuss fuer Stahlbeton*, pp. 23–52.

Wakisaka, Y.; M. Inayoshi; K. Fukui; H. Kosaka; Y. Hotta; A. Kawaguchi and N. Takada (2016). Reduction of heat loss and improvement of thermal efficiency by application of "temperature swing" insulation to direct-injection diesel engines. *SAE International Journal of Engines*, 9(3), 1449–1459.

Walde, R.T. and Khobragade, N.W. (2012). Transient thermoelastic problem of a finite-length hollow cylinder. *Canadian Journal of Science and Engineering Mathematics*, 3(2), 56–60.

Wang, Y.; X. Meng; X. Yang and J. Liu (2014). Influence of convection and radiation on the thermal environment in an industrial building with buoyancy-driven natural ventilation. *Energy and Buildings*, 75, 394–401.

Witek, A.; D. Gawin; F. Pesavento and B. A. Schrefler (2007). Finite element analysis of various methods for the protection of concrete structures against spalling during fire. *Computational Mechanics*, 39, 271–292.

Yarbrough, D.W. (2012). Thermal Insulation for Energy Conservation. In *Handbook of Climate Change Mitigation*, pp. 649–668.

Zhang, W. (2018). The elastic solution of a radial heterogeneous cylinder subjected to non-uniform distributed normal and tangential loads. *Mathematical Problems in Engineering*, 8 pgs.